Organic Electronics 13 (2012) 1250–1254

Contents lists available at SciVerse ScienceDirect

Organic Electronics

journal homepage: www.elsevier.com/locate/orgel

Letter

Anisotropic mobility of small molecule-polymer blend channel in organic transistor: Characterization of channel materials and orientation

Ji Hoon Park [a], Hyunjin Lim [b,c], Hyeonsik Cheong [b], Kyu Min Lee [d], Hyun Chul Sohn [d], Gyubaek Lee [a], Seongil Im [a,*]

[a] Institute of Physics and Applied Physics, Yonsei University, Seoul 120-749, Republic of Korea
[b] Department of Physics, Sogang University, Seoul 121-742, Republic of Korea
[c] Agency for Defense Development, Daejeon 305-152, Republic of Korea
[d] Department of Materials Science and Engineering, Yonsei University, Seoul 120-749, Republic of Korea

ARTICLE INFO

Article history:
Received 13 January 2012
Received in revised form 5 March 2012
Accepted 1 April 2012
Available online 15 April 2012

Keywords:
Anisotropic
Inverter
Solution process
Polymer blend
Organic thin-film transistor

ABSTRACT

We report on the anisotropic properties of solution-processed thin-film transistors (TFTs) fabricated by the vertical flowing of the viscous 6,13-bis(triisopropylsilylethynyl) pentacene (TIPS-pentacene) and isotactic (*i*-) poly-(methyl methacrylate) (PMMA) blend. During film formation processes, lateral crystalline growth of TIPS-pentacene and TIPS-pentacene/*i*-PMMA phase-separation were observed. Such anisotropic crystallization of TIPS-pentacene channel caused anisotropic mobility with respect to the channel orientation, so that it could be used for composing of a logic inverter where two TFTs with different channel orientations were serially connected.

1. Introduction

Organic thin-film transistors (TFTs) have attracted a great deal of attention over last decades, due to their advantage of low cost fabrication [1–16], which brings their research scope to solution processes, such as gravure printing,2 ink jet printing,3 spin coating4 and hollow pen direct writing [5]. Of the many organic materials commercially available, 6,13-bis(triisopropylsilylethynyl)-pentacene (TIPS-pentacene) is an attractive component as an active material for organic TFT in back-plane application in terms of air-stability, and reasonably high mobility [6–8]. Unlike the triethylsilylethynyl anthradithiophene (TES-ADT) which shows isotropic polycrystalline grain shape in general [9], TIPS-pentacene displays strong anisotropic tendency in in-plane crystalline film growth when processed by either ink-jet or drop-casting method; it is because of its strong π-π stacking, which thus hinders the device reproducibility and uniformity [5,10–13].

A possible solution to circumvent these problems was initially suggested by Brown et al. [14]: blending semiconducting small-molecule (TIPS-pentacene) and insulating polymer. Recently, Ohe et al., Kang et al. and Hamilton et al. also blended TIPS-pentacene with poly (α-methylstyrene) (PαMS), which resulted in quite decent mobilities exceeding ~0.1 $cm^2/V\,s$ along with good performance uniformity [6,7,15]. According to them, the improved performance and uniformity of devices were caused by some suppression of anisotropic growth and thermodynamic phase-separation by which two (or three) different layers coexist at top and bottom on a substrate; the phase separation was confirmed by dynamic secondary ion mass spectroscopy or neutron reflectivity technique [6,7,15]. However, since more in-depth understanding on such blended and phase-separated film is still necessary in particular context of actual physical properties and interfaces of such separated semiconducting/insulating layers, we

* Corresponding author. Tel.: +82 2 2123 2842; fax: +82 2 392 1592.
E-mail address: semicon@yonsei.ac.kr (S. Im).

1566-1199/$ - see front matter © 2012 Elsevier B.V. All rights reserved.
http://dx.doi.org/10.1016/j.orgel.2012.04.001

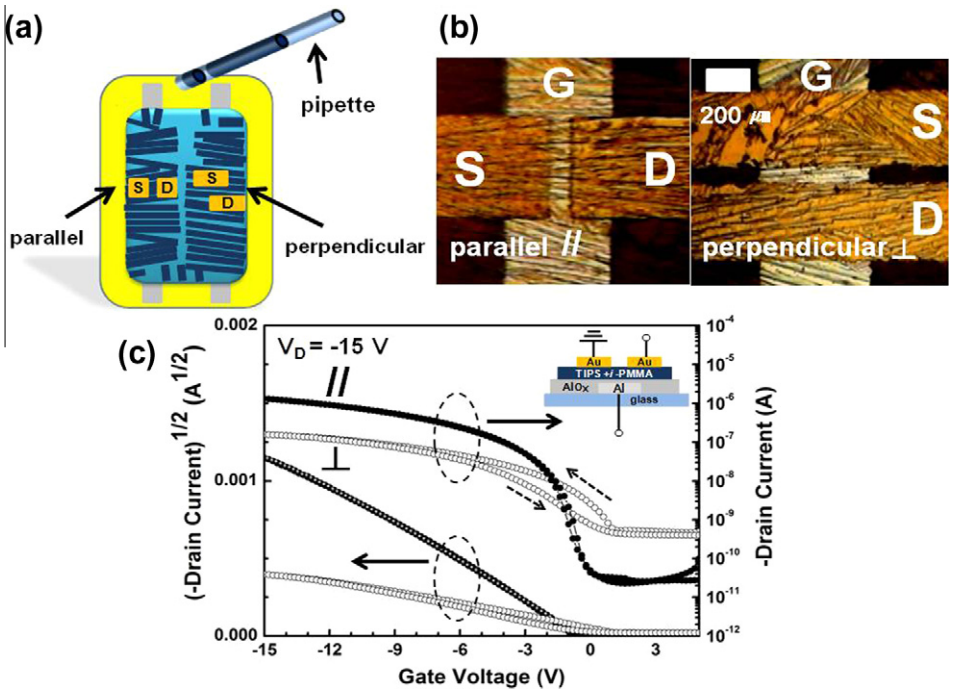

Fig. 1. (a) Schematic of two types of TFT fabricated on TIPS-pentacene/*i*-PMMA film grown by vertical flowing method. TIPS crystalline stripes grow normal to the solution flow. (b) Optical microscope images of the two TFTs fabricated on the stripes (c) $\sqrt{-I_D}$–V_G and $\log_{10}(-I_D)$–V_G plots from parallel(//)- and perpendicular(⊥)-TFTs on sputter-deposited AlO_x gate dielectric (inset). Gate leakage current was <1 nA.

have recently studied such blending and layered-phase-separation. We used a unique deposition technique named "vertical flowing" (Fig 1S and Fig. 1a), where not only the organic semiconductor/insulator separation was noticed

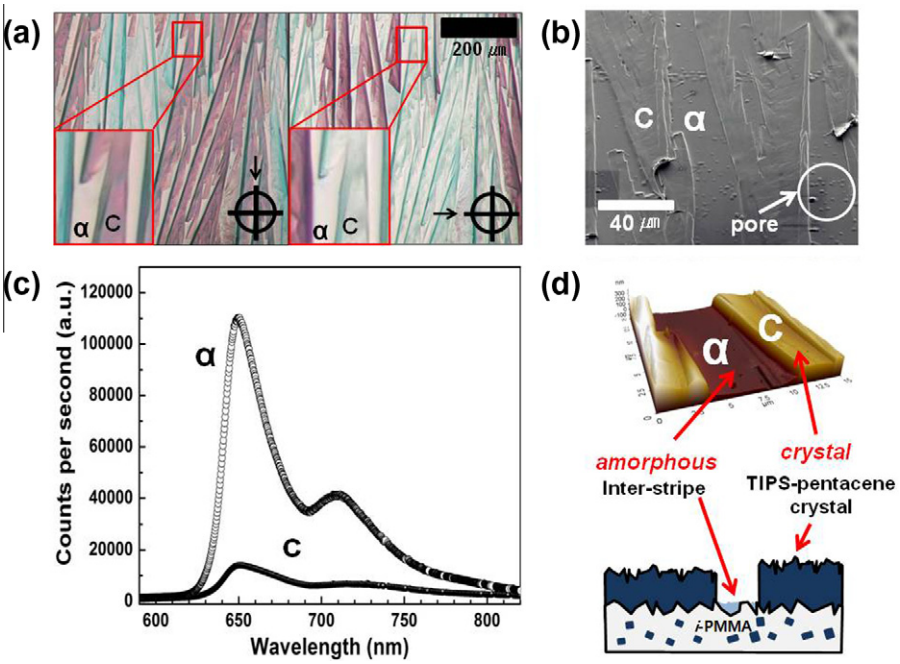

Fig. 2. (a) Polarized optical microscope of aligned TIPS-pentacene/*i*-PMMA blend film on glass with polarizer aligned at 0 (left), and 90° (right). (b) Top-view SEM images of TIPS-pentacene/*i*-PMMA film surface (c) Micro-PL spectra of two different regions show distinct PL spectra. (d) Schematic of possible structure of TIPS-pentacene/*i*-PMMA blend film.

after the process but an anisotropic crystalline growth of organic semiconductor could be also manipulated as perpendicular way to the flowing direction of blended solution [8]. Moreover, in the present study we have fabricated two thin-film transistors (TFTs) with the respective anisotropic channel mobilities, so that a logic inverter can be formed when the two TFTs are serially connected; it was based on our expectation that the anisotropic crystalline growth would induce anisotropic device performance.

2. Experimental section

Above all, a TIPS-pentacene/isotactic poly-(methyl methacrylate) (*i*-PMMA) blend solution (master solution) was prepared according to our previously reported research [8]. It is noticed that the reason we have incorporated *i*-PMMA as insulating polymer is reported elsewhere [16]. Then, for TFTs on glass, a bottom gate electrode of 100 nm-thick Al was thermally evaporated to be patterned on glass (Eagle 2000) through a shadow mask. A 100 nm AlO_x film was deposited by rf magnetron sputtering at room temperature (RT), and hexamethyldisilazane (HMDS) was coated by spin-coating, to be annealed at 110 °C. The master solution was vertically flowed through pipette on the upstanding sputter-deposited AlO_x (100 nm)/patterned gate (G) Al/glass substrate as shown in Fig. 1(a). During drying process of flowed master solution, nucleation and growth were initiated from the edge of the solution strip, since solution evaporation preferably occurred at the edge. After film-drying process for overnight in vacuum, two types of TFTs with two different channel orientations to Au source/drain (S/D) electrode were fabricated by S/D patterning through shadow masks: perpendicular and parallel orientations. Both types of TFTs have nominal channel length (L) and width (W) of 90 μm and 500 μm, respectively. Optical microscope images are shown for the both TFTs in Fig. 1(b). All the electrical measurements of devices such as drain current-gate voltage (I_D–V_G) transfer, inverter voltage transfer characteristics (VTC), were performed with Agilent 4155C semiconductor parameter analyzer in the dark at RT. Environmental scanning electron microscope (SEM) was used for the surface imaging of TIPS-pentacene/*i*-PMMA on SiO_2/p^+-Si.

3. Results and discussion

Fig. 1(c) displays I_D–V_G transfer characteristic of our transistors with two types of S/D arrangement. Here, we

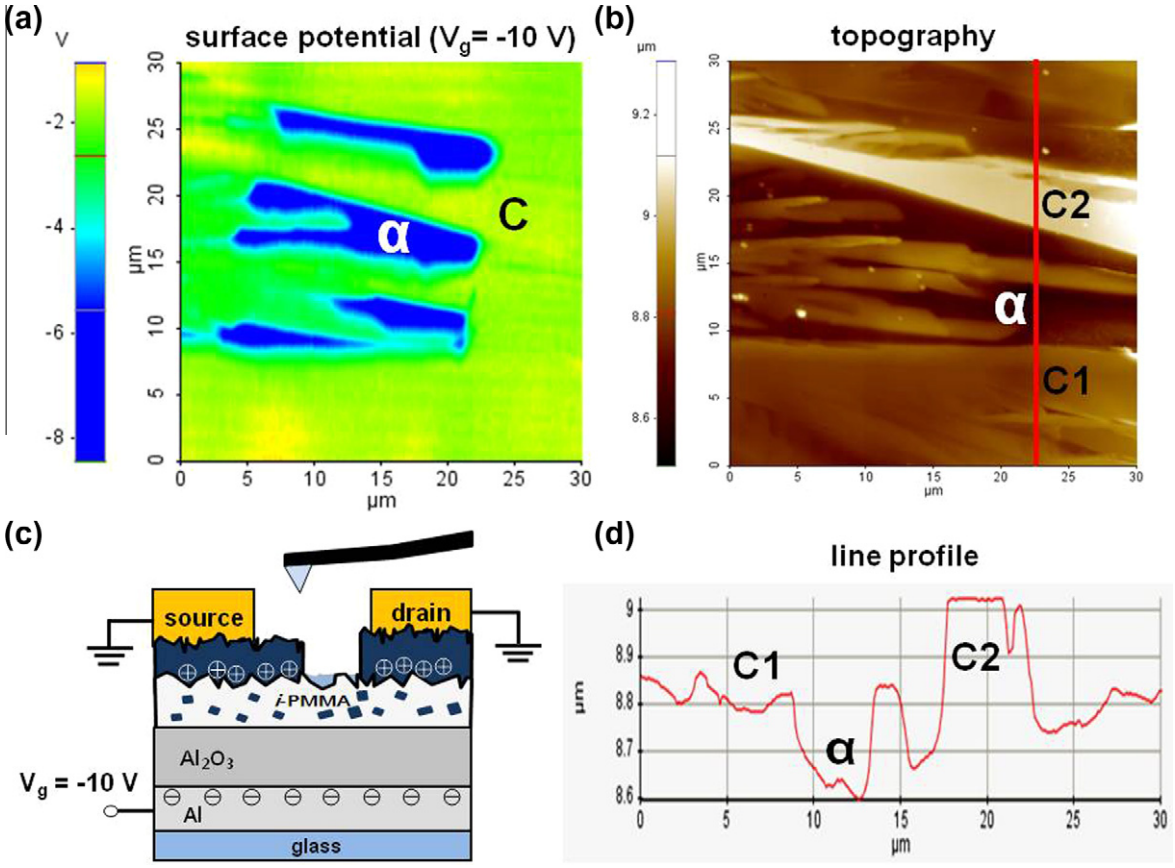

Fig. 3. (a) Surface potential image mapped by SKPM in a TIPS-pentacene channel region on *i*-PMMA/AlO_x under −10 V of V_G vs. (b) AFM topography image of corresponding area. (c) Schematics of our SKPM measurement. (d) Line profile was also obtained from (b) AFM topography along with red line. C2 region is brighter than C1.

assign the first type of TFT as 'parallel', and the other type as 'perpendicular' by considering the growth orientation of TIPS pentacene channel. The extracted saturation mobilities were 0.3 (filled circle) and 0.03 cm^2/V s (open circle) for parallel- and perpendicular-oriented TIPS pentacene channel at a drain voltage of −15 V, respectively. The parallel-type TFT exhibited quite good uniform performance (∼±10% standard variation in saturation mobility) as reported previously,[8] however, the perpendicular-type TFT showed large variation in saturation mobility from 0.005 to 0.03 cm^2/V s, presumably, due to complicated current path in channel region. The perpendicular-type TFT showed inferior sub-threshold swing, larger gate-hysteresis, and higher off-current, which might be attributed to larger G/S-D overlap area. The different I_D values from the two devices are certainly related to the anisotropic orientation of our TIPS pentacene crystalline channel, based on the fact that channel L and W are identical in both types of TFT. We thus wanted to examine the anisotropic lateral structures of our blended film (TIPS-pentacene/*i*-PMMA) in more detail, using polarized optical microscope, microphotoluminescence (PL) spectroscopy [17–19], and scanning kelvin probe microscope (SKPM) [20].

Fig. 2(a) displays the images from polarized light microscopy that we used to observe any details in unilaterally-grown crystalline channel. Any crystalline region showed brightness change by changing the in-plane angle of incident polarized light as seen in the region, C (as zoomed in the small square regions). However, we also found another region, α (void or amorphous) which keeps the same brightness even after 90 ° rotation of incident polarized light. This does mean that our crystalline channel contains some noncrystalline region (between stripe-like TIPS-pentacene crystallites), which should block or complicate the current path in perpendicular-type TFT lowering the I_D. Such noncrystalline inter-stripe regions were also found to have small pores, as shown in top-view SEM image of Fig. 2(b), indicated by circle. These pores were also observed from *i*-PMMA rich layer beneath the α-region by cross-section transmission electron microcopy (TEM) (Fig. 1S). So, these α-regions can hardly be crystalline.

More interesting to note is that these α-regions display strong light emission caused by ultraviolet light-induced excitation (see the Fig. 2S). According to our micro-PL results from channel area (Fig. 2(c)), the α-region exhibits 7 times stronger red PL intensity (at 650 nm) than C-region does. The spatial resolution of micro-PL measurement was less than 1 μm and the beam footprint was applied onto the α- and C- regions of atomic force microscope (AFM) image (see the inset of Fig. 2(d)). Since the α-regions have lower topography than C- regions as shown in AFM topography and also show intense PL emission, it is presumed that the α-region is void or exists as thin amorphous on *i*-PMMA layer which may contain some TIPS-pentacene molecules embedded as PL sources (see Fig. 2(d)), while C-regions are covered by crystalline TIPS-pentacene films.[21] It is likely that while most of the TIPS-pentacene molecules segregate toward the surface of blending film for TIPS-pentacene film-formation by π–π stacking, some uninvolved TIPS-pentacene molecules may be solidified inside *i*-PMMA film.

The topographical height difference between α- and C-region was again confirmed by SKPM measurement which was directly implemented on a TFT under a bias condition: −10 V of V_G and $V_S = V_D = 0$ V with ground (see the measurement scheme illustrated in Fig. 3(c)). As shown in the 2-dimensional potential map of Fig. 3(a), large contrast was revealed due to surface potential difference between α- and C-region under −10 V gate bias. Since hole charge accumulation by the negative bias should be only at the TIPS-pentacene channel which is located at the TIPS-pentacne/*i*-PMMA interface, the voltage effectively drops through thickness of the *i*-PMMA/AlO_x double dielectric layer beneath TIPS-pentacene; therefore the potential of TIPS-pentacene surface (C-region) must be small; it appeared here, to be ∼−2 V. According to our mapping, the inter-stripe α-region showed deep contrast evidencing that it still keeps high surface potential values (−7 ∼ −8 V). This means that the corresponding area has no hole charge accumulation but only floating voltage; the results indicate that the region is void without TIPS-pentacene or has very thin amorphous film covering the *i*-PMMA/AlO_x dielectric. AFM topographic scan on the same area was not exactly the same as that of SKPM but certainly showed similar contrast in Fig. 3(b). Line scan in AFM was also obtained to show the height difference values (as ∼0.21 μm) between C- and α-region as shown in Fig. 3(d).

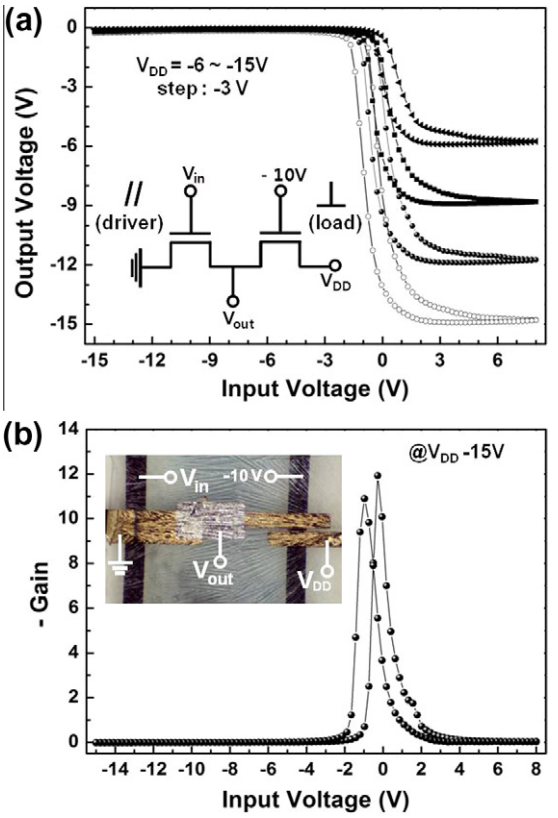

Fig. 4. (a) Static behavior of our resistance–load inverter with varying value of V_{DD}. Two TFTs, perpendicular and parallel TFTs, were combined. (b) At V_{DD} of −15 V, the VTC curve of our inverter displays voltage gain up to ∼12. Inset shows top-view of inverter with Al interconnects.

Based on aforementioned understanding and knowledge about physical identity of inter-stripe region, anisotropic TIPS-pentacene crystalline growth during film formation or phase separation, and anisotropic field mobility of TFTs, we finally fabricated a logic inverter which consists of driver and load as parallel- and perpendicular-type TFTs, respectively as shown in the inset photo of Fig. 4(b). When input voltage was swept at the gate of parallel-type TFT (driver), our inverter response to output voltage appeared very clear between −15 V ("high") and +8 V ("low") under various supply voltages (V_{DDs} = −6, −9, −12, and −15 V) and a fixed −10 V of load TFT (perpendicular-type) in the voltage transfer curves of Fig. 4(a). The observed hysteresis might be attributed to the gate hysteresis from perpendicular-type TFT, which was shown in the transfer curve of Fig. 1(c). In respect of voltage gain, the inverter shows a maximum value of ∼12 at V_{DD} of −15 V (Fig. 4(b)).

4. Conclusion

In summary, we have fabricated solution-processed TIPS-pentacene TFTs by vertical flowing of the viscous TIPS-pentacene and *i*-PMMA blend. Since anisotropic crystallization of TIPS-pentacene and TIPS-pentacene/*i*-PMMA phase-separation appeared during such film formation processes, we could observe different field mobilities from parallel- and perpendicular-type TFTs where the perpendicular type showed lower I_D current due to inter-stripe-regions as obstacles to the current path. When the two types of TFTs were serially connected, a logic inverter with quite a good voltage gain was formed due to the anisotropic mobility behavior.

Acknowledgements

The authors acknowledge the financial support from KOSEF (NRL program, No. 2011-0000375), the 21st Century Frontier R&D Program funded by the MKE (Information Display R&D center, F0004022-2011), and Brain Korea 21 Project. H. Cheong thanks the Midcareer Researcher Program through NRF Grant funded by the MEST (No. 2011-0017605).

Appendix A. Supplementary data

Supplementary data associated with this article can be found, in the online version, at http://dx.doi.org/10.1016/j.orgel.2012.04.001.

References

[1] C.C. Dimitrakopoulos, P.R.L. Malenfant, Adv. Mater. 14 (2002) 99.
[2] H. Yan, Z. Chen, Y. Zheng, C. Newman, J.R. Quinn, F. Dötz, M. Kastler, A. Facchetti, Nature 457 (2009) 679.
[3] M. Lada, M. Starink, M. Carrasco, L. Chen, P. Miskiewicz, P. Brookes, M. Obarowska, D. Smith, J. Mater. Chem. 21 (2011) 11232.
[4] Y.-H. Kim, Y.U. Lee, J.-I. Han, S.-M. Han, M.-K. Han, J. Electrochem. Soc. 154 (2007) H995.
[5] R.L. Headrick, S. Wo, F. Sansoz, J.E. Anthony, Appl. Phys. Lett 92 (2008) 063302.
[6] J. Kang, N. Shin, D.Y. Jang, V.M. Prabhu, D.Y. Yoon, J. Am. Chem. Soc. 130 (2008) 12273.
[7] R. Hamilton, J. Smith, S. Ogier, M. Heeney, J.E. Anthony, I. McCulloch, J. Veres, D.D.C. Bradley, T.D. Anthopoulos, Adv. Mater. 21 (2009) 1166.
[8] J.H. Park, K.H. Lee, S. Mun, G. Ko, S.J. Heo, J.H. Kim, E. Kim, Seongil I.m., Org. Electron. 11 (2010) 1688.
[9] K.C. Dickey, J.E. Anthony, Y.L. Loo, Adv. Mater. 18 (2006) 1721.
[10] J. Chen, C.K. Tee, M. Shtein, D.C. Martin, J. Anthony, Org. Electron. 10 (2009) 696.
[11] O. Ostroverkhova, D.G. Cooke, F.A. Hegmann, R.R. Tykwinski, S.R. Parkin, J.E. Anthony, Appl. Phys. Lett 89 (2006) 192113.
[12] C.W. Sele, B.K.C. Kjellander, B. Niesen, M.J. Thornton, J.B.P.H. van der Putten, K. Myny, H.J. Wondergem, A. Moser, R. Resel, A.J.J.M. van Breemen, N. van Aerle, P. Heremans, J.E. Anthony, G.H. Gelinck, Adv. Mater. 21 (2009) 4926.
[13] J.A. Lim, H.S. Lee, W.H. Lee, K. Cho, Adv. Funct. Mater. 19 (2009) 1515.
[14] B.A. Brown, J. Veres, R.M. Anemian, R. Williams, S.D. Ogier, S.W. Leeming, W.O. Pat., 2005/055248, (2005); B.A. Brown, J. Veres, R.M. Anemian, R. Williams, S.D. Ogier, S.W. Leeming, US Pat., 7576208 B2, (2009).
[15] T. Ohe, M. Kuribayashi, R. Yasuda, A. Tsuboi, K. Nomoto, K. Satori, M. Itabashi, J. Kasahara, Appl. Phys. Lett. 93 (2008) 053303.
[16] J.H. Park, D.K. Hwang, J. Lee, S. Im, E. Kim, Thin Solid Films 515 (2007) 4041.
[17] J.S. Lee, H. Lim, K. Ha, H. Cheong, K.B. Yoon, Angew. Chem. Int. Ed. 45 (2006) 5288.
[18] S.S. Kim, Y.-J. Kim, G.-C. Yi, H. Cheong, J. Appl. Phys. 106 (2009) 094310.
[19] H. Lim, H. Cheong, S. Choi, Y.N. Choi, J.S. Lee, J. Korean Phys. Soc. 58 (2011) 1035.
[20] T. Hallam, M.J. Lee, N. Zhao, I. Nandhakumar, M. Kemerink, M. Heeney, Iain McCulloch and Henning Sirringhaus, Phys. Rev. Lett. 103 (2009) 256803.
[21] L. Schmidt-Mende, A. Fechtenkötter, K. Müllen, E. Moons, R.H. Friend, J.D. MacKenzie, Science 293 (2001) 1119.